Econ. Environ. Geol.
Vol. 29, No. 3, p. 345-355, 1996.

# Effectiveness of the Electrode Arrays for Delineating 2-D Subsurface Structure

**Jong-Ryeol Yoon* and Kiehwa Lee***

ABSTRACT : The effectiveness of various electrode configurations in horizontal mappings and 1-D inversions of vertical sounding data for delineating 2-D structures was studied. Apparent resistivity values of three point, dipole-dipole, Wenner, and Schlumberger mappings were simulated for such structures as vertical dyke, tabular prism, buried vertical fault, ramp and complex structure by finite difference method (FDM) and they were compared with each other. Also 2-D cross sections for three structures obtained by interpolation of 1-D inverted sounding data in terms of three layers were compared for Schlumberger and Wenner arrays. On these cross sections, horizontal and vertical resistivity interfaces of the 2-D structures are revealed relatively clearly. Apparent resistivity curves of Schlumberger mapping show vertical resistivity discontinuities very well. On the whole, Schlumberger array is superior to the other arrays in electric sounding as well as mapping. This study clearly indicates that interpretations of 2-D structures based on 1-D inversion are possible.

## INTRODUCTION

Electric exploration data are often interpreted by one-dimensional (1-D) layered model. A number of studies on interpretation of electric sounding data using layered model have been made (Mooney *et al.*, 1966; Inman, 1975; Zohdy, 1989). However, in many cases, 1-D interpretation may be very difficult to incorporate with the 2-D or 3-D subsurface structure. Since the late 1970s, interpretation techniques based on 2-D model have been developed for dipole-dipole array surveys (Dey and Morrison, 1979; Smith and Vozoff, 1984; Tripp *et al.*, 1984; Sasaki, 1989). However, 2-D inversions require much computing time and large computer memory. Therefore, there arise needs to study to what extent 1-D interpretation can elucidate the real 2-D subsurface structure (Beard *et al.*, 1991) and what electrode configurations are more effective in mapping and sounding the 2-D structure.

In this study, five simple 2-D subsurface structures were simulated. Each 2-D subsurface structure was divided into $200 \times 15$ blocks and at every nodal point electric potentials were calculated using finite difference method described by Dey and Morrison (1979). These calculated potentials were assumed as observed data in sounding and mapping.

* Department of Geological Sciences, Seoul National University, Seoul, 151-742, Korea

Twenty five soundings and forty mappings were calculated at various nodal points over each structure. Soundings were interpreted by iterative least square inversion approach (Inman, 1975; Lines and Treitel, 1984; Constable *et al.*, 1987) assuming a three layered earth. To calculate kernel in inversion procedure, ZHANKS FORTRAN subroutine (Anderson, 1979) was used. The 2-D cross-sections for Wenner and Schlumberger arrays were obtained from interpolation of these 1-D inverted data and compared with each other. Also, apparent resistivity curves for three point, dipole-dipole, Wenner, and Schlumberger mappings were compared. All the numerical calculations were performed by Seoul National University Alliant FX/2812 parallel supercomputer. The flow chart of data processing of this study is shown in Fig. 1.

## FINITE DIFFERENCE METHOD

In 2-D resistivity modeling, the resistivity depends on two coordinates (x and z). But, as the current source is point, the electric potential will also depend on the third coordinate, y, i.e., strike direction. In order to remove the potential's dependence on the strike direction, Fourier cosine transform may be applied since the potential is an even function of y. After applying the transform, discretization of the subsurface into the mesh of rectangular elements is performed. To obtain the potential at each node,

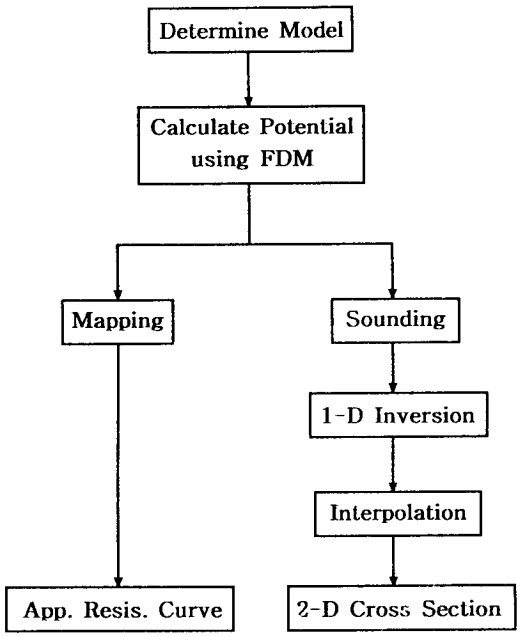


**Fig. 1.** Flow chart of data processing.

transformed differential equation is expanded to finite difference equation.

Transformed potential and normal component of the current must be continuous across each interface of the different boundary. In this study, the mixed boundary condition proposed by Dey and Morrison (1979) was imposed. This condition produces better numerical solutions than the classical ones (Dirichlet or Neumann). The set of finite difference equations satisfying the mixed boundary condition can be applied to all nodes and these equations can be written in matrix form or symbolically, as

$$C\varphi = S\varphi$$

where $\varphi$ is the transformed potential vector and **C** is the capacitance matrix. **S** is the source vector and is all zero except source locations. Capacitance matrix is positive definite (Varga, 1962) and remains unaltered for different and multiple source locations. Hence for the different source locations of the same model, only one calculation is needed. In this study, matrix equation was solved by Gauss elimination algorithm for banded symmetric matrix.

The inverse cosine transform of the potential was performed by numerical integration using trapezoidal rule. Then, the electric potential, V (x, y, z), can be obtained from the set of (x, $K_y$, z) for several optimal values wave number in y direction, $K_y$. But singularity occurs in the solution of any elliptic

**Table 1.** Values of wave numbers in y direction ($K_y$).

| $K_1$ | $K_2$ | $K_3$ | $K_4$ | $K_5$ |
|---|---|---|---|---|
| 0.0001 | 0.001 | 0.01 | 0.04 | 0.12 |
| $K_6$ | $K_7$ | $K_8$ | $K_9$ | $K_{10}$ |
| 0.2 | 0.5 | 0.8 | 1.28 | 3.5 |

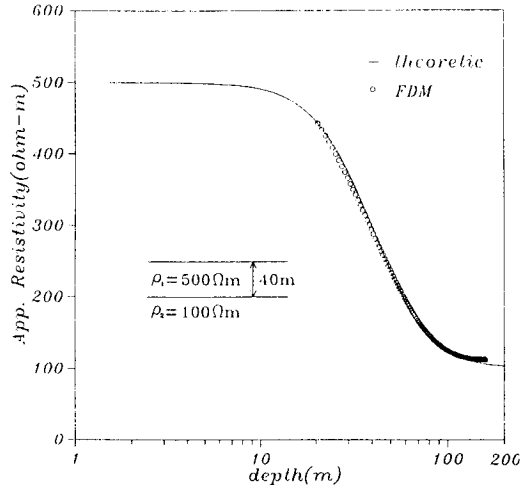


**Fig. 2.** Test of FDM solution for Schlumberger sounding.

partial differential equation for which the forcing function is not smooth (Lowry *et al.*, 1989). Hence, the potential in the (x, $K_y$, z) domain has singularity at zero $K_y$ value and numerical integration causes some errors. The number of $K_y$ values also influences errors of inverse transform. Since the large number of $K_y$ values increases computing time, ten inequally spaced optimal $K_y$ values were used (Table 1) in this study.

In order to estimate the accuracy of finite difference method described above, a two layer model was simulated. The resistivity of the top layer of thickness 40m was assumed to be 500 $\Omega$m and that of the bottom layer to be 10m. It is assumed that a Schlumberger sounding was performed over the top layer. The results of Schlumberger sounding is shown in Fig. 2. The theoretical response (Telford, 1976) for the two layer model is shown by the curve with solid line and FDM solution with circles. The numerical results differ from the theoretical solution within 6%.

## ITERATIVE LEAST SQUARES INVERSION

The purpose of inversion is extracting the model parameters from an attempted fit of the model

response to the observed data. Accordingly, model response is calculated and compared with the observation, and the model parameters are then modified in a way which will better fit the observation. If the model response is a linear function of the model parameters, the model response can be represented by the first-order Taylor expansion. Then Jacobian matrix which consists of partial derivatives of the model response with each model parameter has constant elements. Hence, only one modification of model parameters is needed.

But the problem of the electric sounding over a layered subsurface is nonlinear in the unknown parameters, such as the resistivity and thickness of each layer. In the case of nonlinear problem, model parameters are updated iteratively until the obtained error of each step is not less than the error of previous step. Finally, we can get the model parameters having least squares error.

In electric sounding problem, since the layer resistivities and thicknesses must have positive values, logarithms of those model parameters are taken (Vozoff and Jupp, 1975). Furthermore, in order to speed the convergence of model parameter solutions, scaling of Jacobian matrix is needed

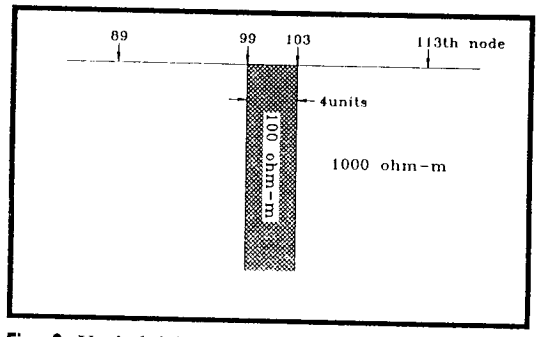


**Fig. 3.** Vertical dyke model.

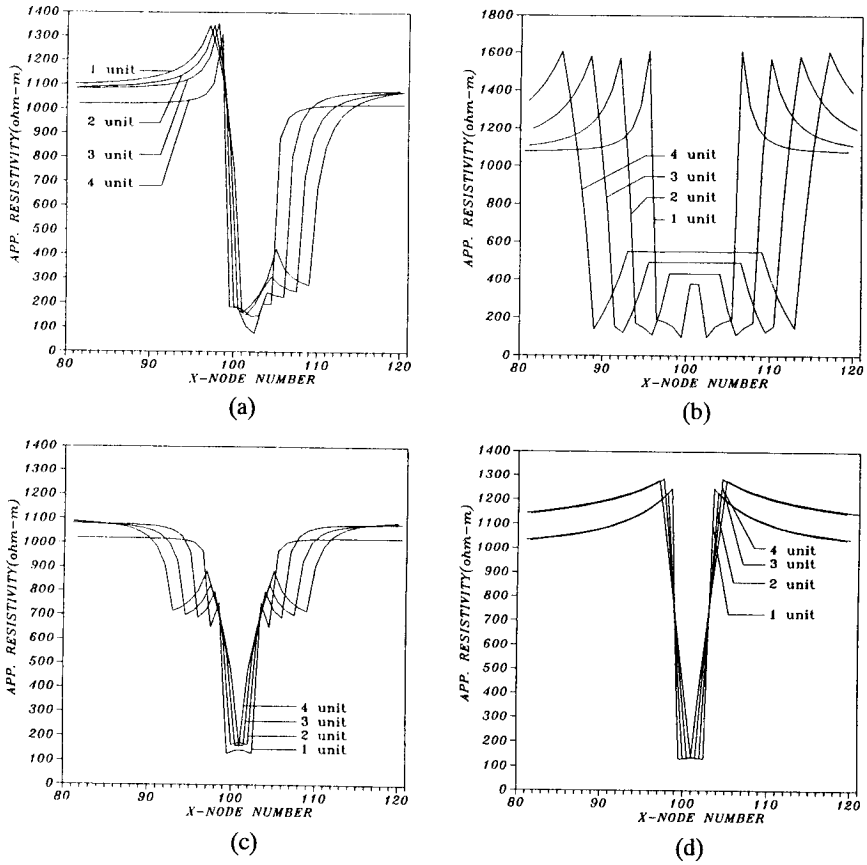


**Fig. 4.** Apparent resistivity curves of electric mappings with different potential electrode separations for vertical dyke model; (a) Three point array (b) Dipole-dipole array (c) Wenner array (d) Schlumberger array.

(Lines and Treitel, 1984). The element $d_{ii}$ of scaling matrix **D** which is diagonal matrix, is equal to the root mean sum (r.m.s.) of square of the elements in the i-th column of the unscaled Jacobian matrix. The resulting solution vector must then be rescaled.

In this study, matrix inversion was performed by use of singular value decomposition (Press *et al.*, 1986) to avoid singularity in the stage of updating model parameters.

## 2-D MODEL SIMULATION

In this study, five 2-D subsurface models were examined; (1) vertical dyke, (2) buried vertical fault, (3) tabular prism, (4) ramp, and (5) complex structure which includes vertical fault and three layers. For each model, results of electric mappings performed at interval of one unit at forty points for Schlumberger, Wenner, three point, and dipole-dipole arrays were compared with each other.

In the case of electric sounding, Schlumberger and Wenner configurations which have been most commonly used were investigated. Electric soundings were performed at twenty two or twenty three nodal points at interval of one unit. The inverted values of sounding data in terms of three layer were interpolated in $25 \times 25$ grids by minimum curvature method. These interpolated data were expressed on 2-D cross section. One block of each cross section corresponds to one unit of the simulated model in both x and z direction.

### Vertical Dyke

The vertical dyke shown in Fig. 3 extends from surface downward to infinity. The width of dyke is 4 units and the resistivity of the dyke is 100 ohm-m, while that of the surrounding rock is 1000 ohm-m. Since this model is symmetric, the potential was calculated using the principle of reciprocity, which results in saving computation time.

Fig. 4 shows the apparent resistivity curves of four different electrode arrays with various potential electrode separations. Since the three point array is not symmetric, its curve is not symmetric either. But the other apparent resistivity curves show the symmetry. For dipole-dipole array, the current electrodes are not located symmetrically about the potential electrodes, and its curve spreads as potential electrode separation increases.

All the apparent resistivity curves show sharp peaks near the resistivity boundary. These peaks are due to image charge. Since this image charge amplifies the potential difference, the apparent resistivity becomes large near the resistivity boundary. Schlumberger and Wenner mappings represent the dyke model more clearly than the other arrays. But Schlumberger mapping is superior to the Wenner mapping. Fig. 4 also shows that the closer the potential electrode separation is, the more clearly the vertical resistivity boundary is represented.

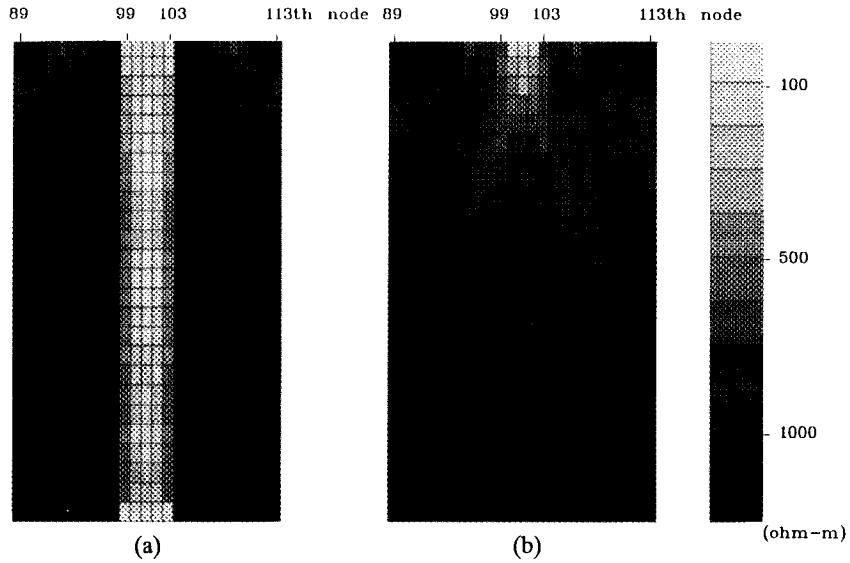


**Fig. 5.** 2-D cross sections for vertical dyke model; (a) Schlumberger array (b) Wenner array.

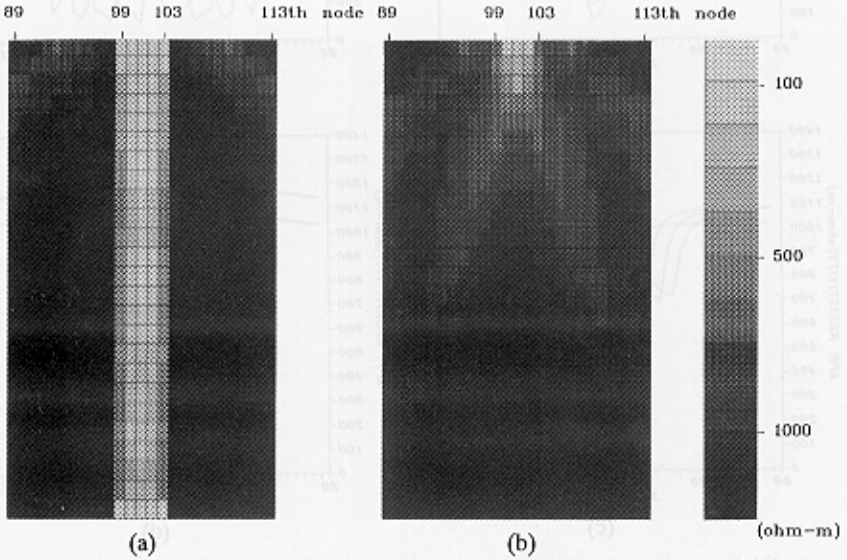


**Fig. 5.** 2-D cross sections for vertical dyke model; (a) Schlumberger array (b) Wenner array.

The 2-D cross sections of Schlumberger and Wenner arrays are shown in Fig. 5. The 2-D cross section of Schlumberger array shows the infinite vertical dyke model clearly. But Wenner array does not represent the vertical resistivity boundary clearly. Because the potential electrode separation increases with current electrode separation in Wenner sounding, the apparent resistivity is more affected by the surrounding medium than in Schlumberger sounding. Thus Wenner soundings represent poorly the vertical dyke model having relatively small width in comparison to depth extent. It is obvious that Schlumberger array is also superior to Wenner array in case of electric sounding.

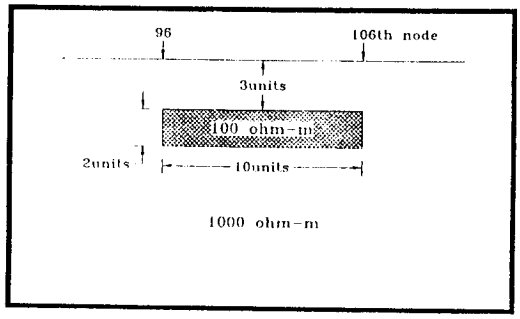


**Fig. 6.** Tabular prism model.

### Tabular Prism

The simulated tabular prism model is shown in Fig. 6. The 100 ohm-m prism is buried 3 units deep in a 1000 ohm-m half-space. The prism is 2 units thick and 10 units wide. Since this model is symmetric like the vertical dyke model, the potential was calculated using the principle of reciprocity.

Fig. 7 shows the results of the electric mappings. In case of the three point and Wenner mappings, the apparent resistivity curves for small separations of

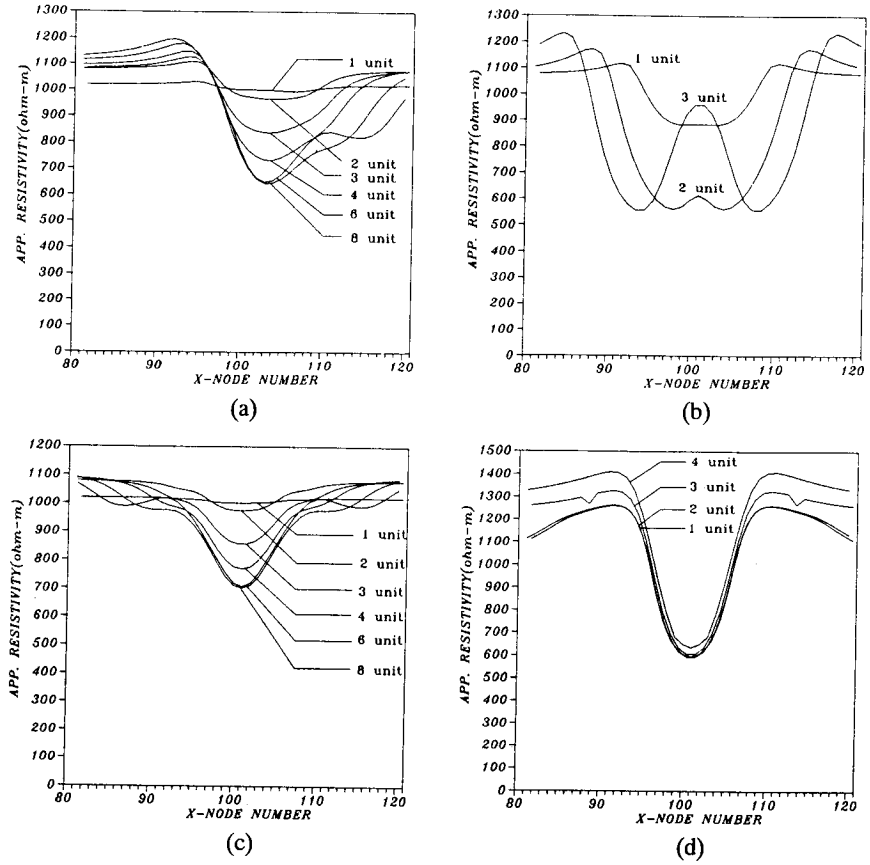


**Fig. 7.** Apparent resistivity curves of electric mappings with different potential electrode separations for tabular prism model; (a) Three point array (b) Dipole-dipole array (c) Wenner array (d) Schlumberger array.

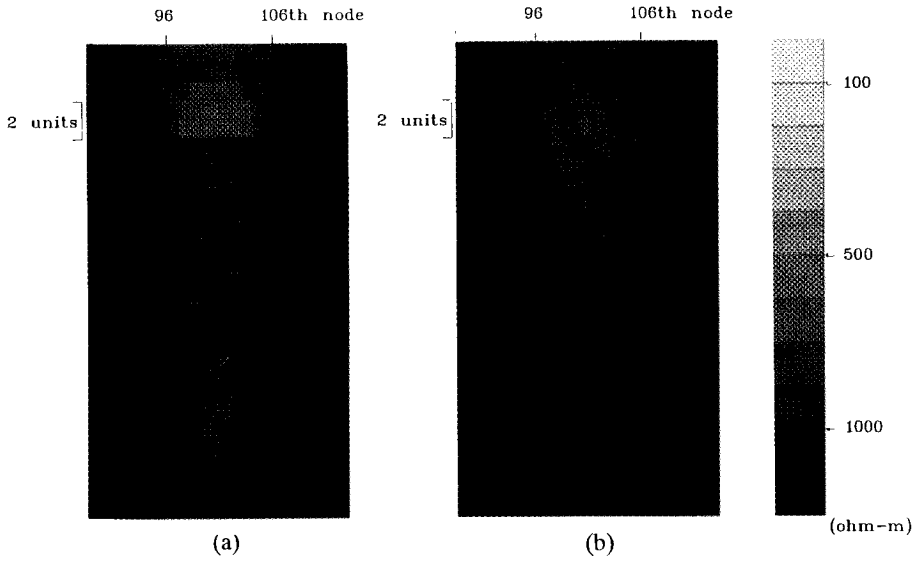


**Fig. 8.** 2-D cross sections for tabular prism model; (a) Schlumberger array (b) Wenner array.

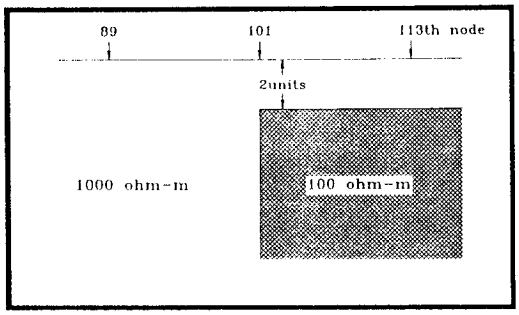


**Fig. 9.** Buried vertical fault model.

potential electrodes (1~2 units) are nearly flat because the current electrode distance is not large enough to represent the tabular prism buried 3 units deep. All the mapping curves do not show the sharp peaks not like the case of the vertical dyke, because the resistivity boundary is not exposed to the surface. For this model, Schlumberger and Wenner arrays are superior to the others.

The 2-D geoelectric sections are shown in Fig. 8. Schlumberger sounding shows the prism clearly. But above the top surface of the prism, a relatively low resistivity zone appears. This low resistivity zone results from the lack of shallow depth information. Usually, the separation of current electrode is very large compared to that of potential electrode in Schlumberger array. Since the potential electrode separation is 1 unit and the current electrode separation must increase from 20 units in this study, and the information of the shallow depth is lacking.

If the block is divided more finely, such low resistivity zone may be removed. However, since the computing time increases exponentially as the number of blocks increases arithmetically, it is important to determine the proper number of blocks for each model. It is also noted that the long plug appears below the prism. Wenner sounding does not show the resistivity boundary clearly.

### Buried Vertical Fault

The buried vertical fault model is shown in Fig. 9. The vertical edge of the fault block is located at the 101th node and is assumed to extend downward infinitely. The horizontal interface is 2 units deep. The resistivity of the fault block is 100 ohm-m and that of the surrounding medium is 1000 ohm-m. Since this model is not symmetric, the potential was calculated at all nodal points.

Fig. 10 shows that Schlumberger mapping represents the buried vertical fault clearly. The other arrays do not show the vertical boundary clearly. In Schlum- berger mapping, the potential electrode separation seems to matter little for this model.

In Fig. 11, it is shown that Wenner sounding fails to represent the vertical fault boundary as clearly as Schlumberger sounding. As mentioned before, Schlumberger sounding does not show the horizontal fault boundary because of the limited number of

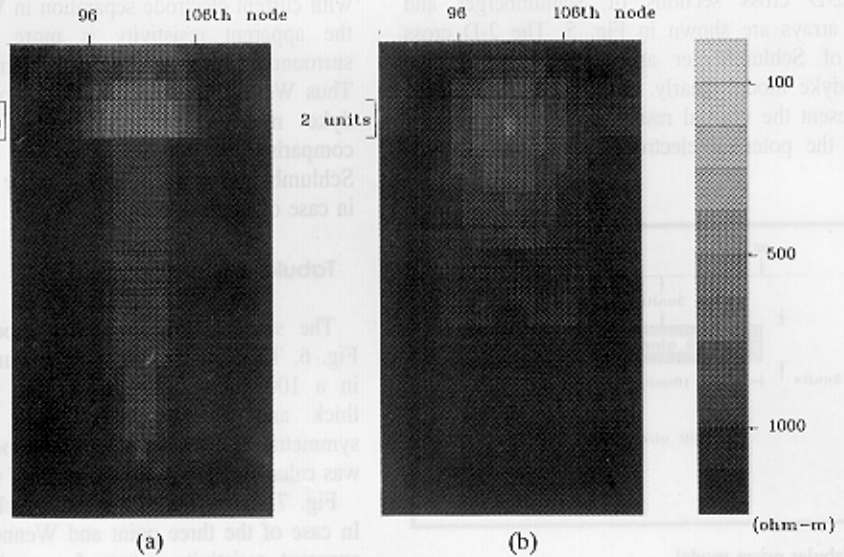


**Fig. 8.** 2-D cross sections for tabular prism model; (a) Schlumberger array (b) Wenner array.

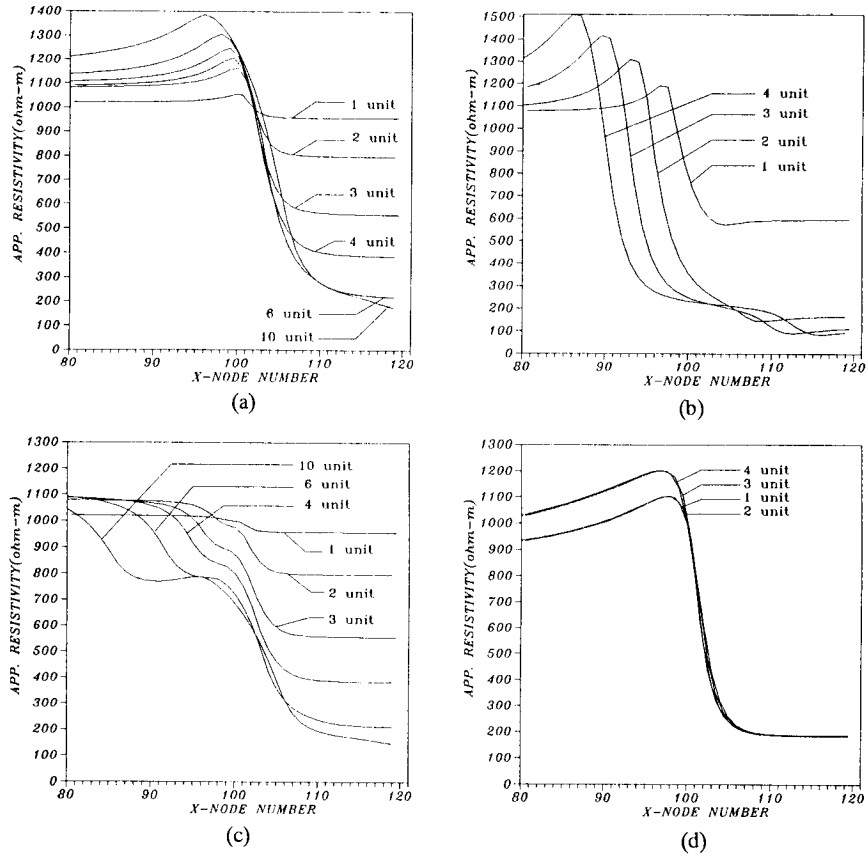


**Fig. 10.** Apparent resistivity curves of electric mappings with different potential electrode separations for buried vertical fault model; (a) Three point array (b) Dipole-dipole array (c) Wenner array (d) Schlumberger array.

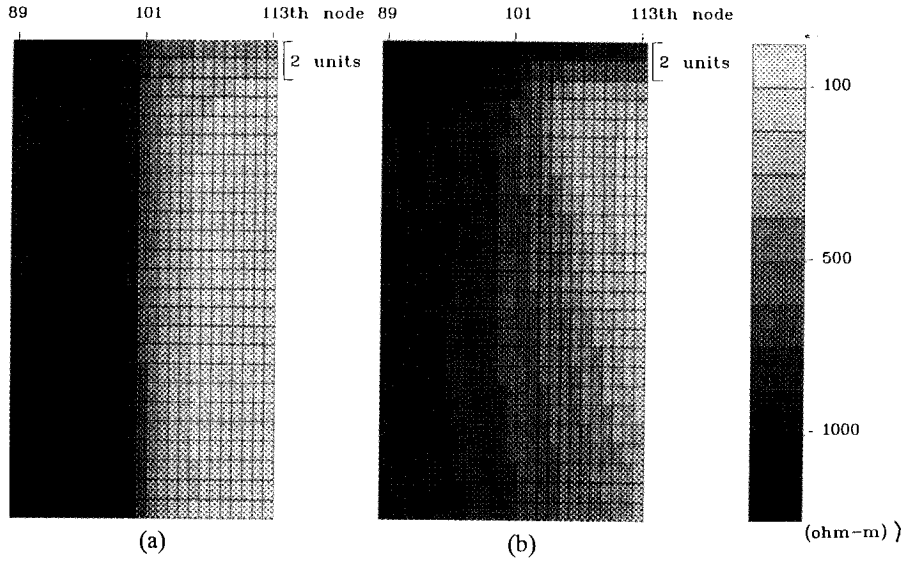


**Fig. 11.** 2-D cross sections for buried vertical fault model; (a) Schlumberger array (b) Wenner array.

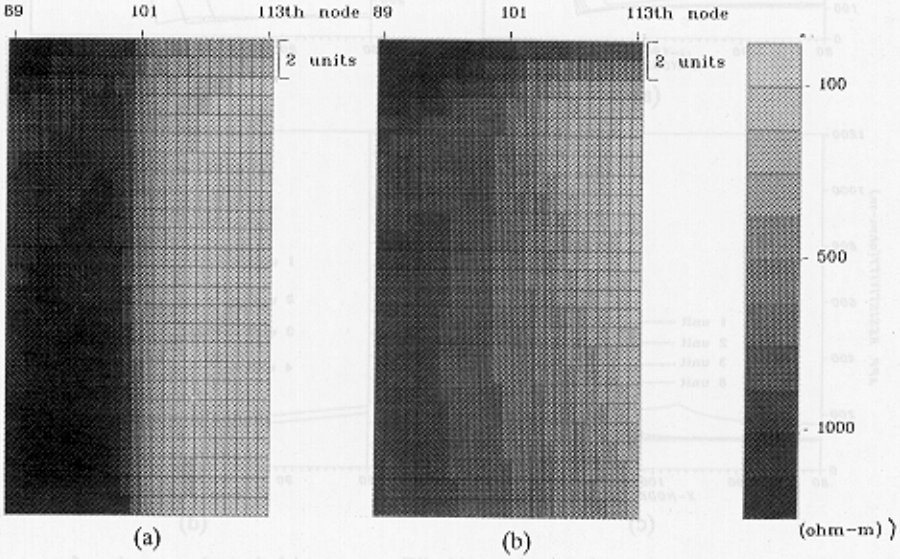


**Fig. 11.** 2-D cross sections for buried vertical fault model; (a) Schlumberger array (b) Wenner array.

dividing blocks. On the other hand, Wenner sounding shows the horizontal boundary relatively well. However, if we increase the number of divided blocks, Schlumberger sounding may show the shallow horizontal boundary as clearly as the vertical boundary.

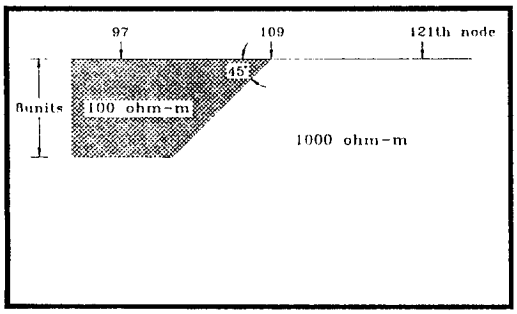


**Fig. 12.** Ramp model.

## Ramp

Fig. 12 shows the ramp model. The ramp angle is 45 degrees to the surface and the vertical thickness is 8 units. The corner of the ramp is located at the 109 th node. The rock above the ramp has the resistivity of 100 ohm-m while that of the surrounding rock is 1000 ohm-m.

In Fig. 13, we can see that Schlumberger mapping shows a very large apparent resistivity at the corner of the ramp. It is because that the resistivity discontinuity is exposed to the surface like the vertical dyke model. All the other electric mappings fail to represent the ramp structure as clearly as Schlumberger mapping.

The center of the cross section in Fig. 14 is at the 109th node. It is shown that Wenner sounding better represents the ramp structure than Schlumberger sounding. It seems that Wenner sounding is more sensitive to the variation of the resistivity with depth

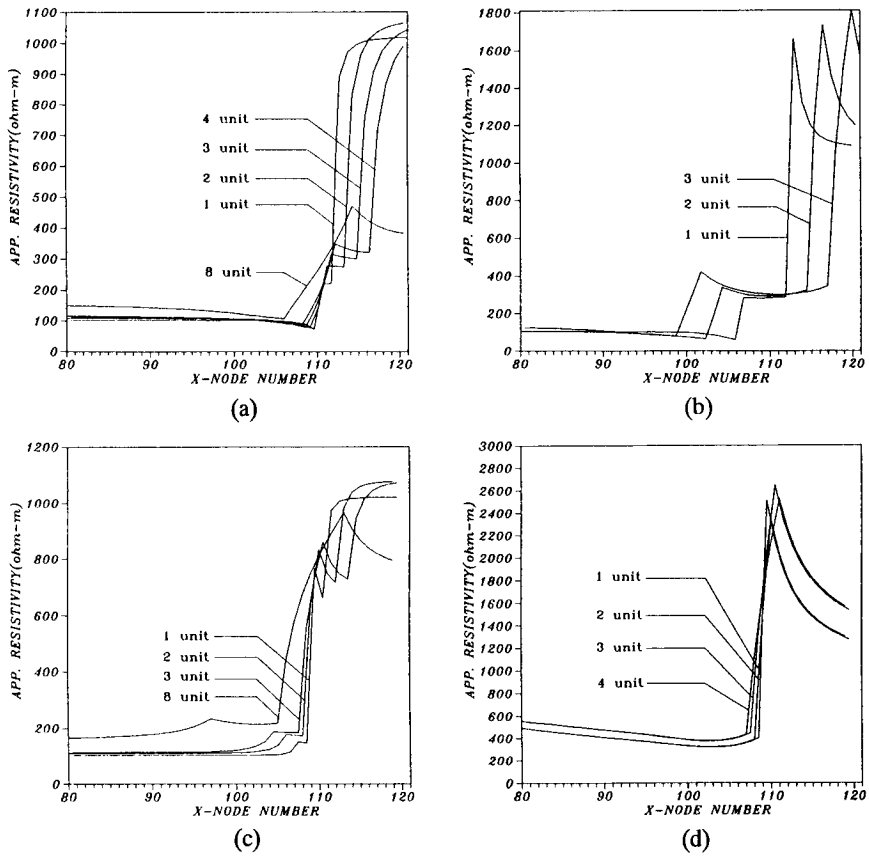


**Fig. 13.** Apparent resistivity curves of electric mappings with different potential electrode separations for ramp model; (a) Three point array (b) Dipole-dipole array (c) Wenner array (d) Schlumberger array.

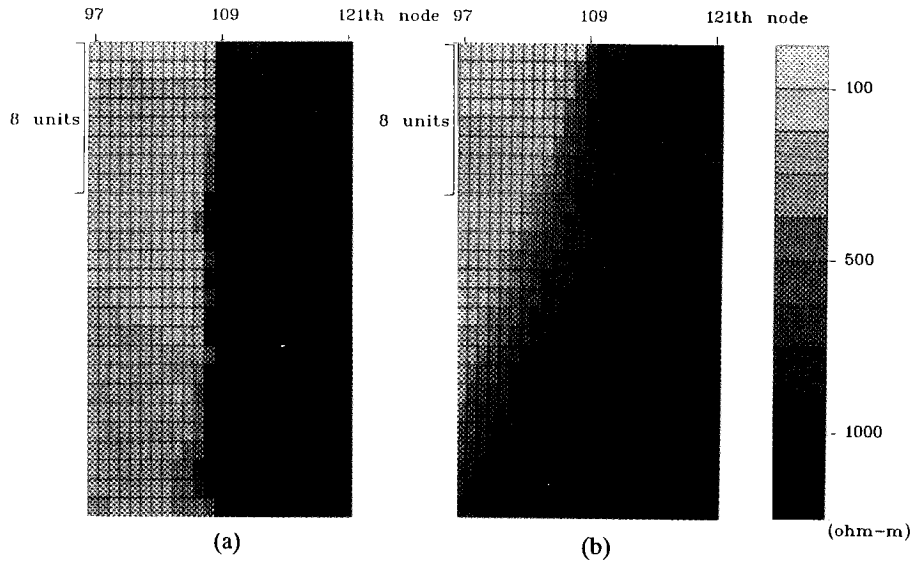


**Fig. 14.** 2-D cross sections for ramp model; (a) Schlumberger array (b) Wenner array.

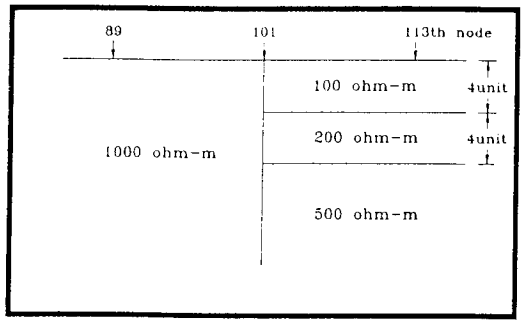


**Fig. 15.** Complex model.

than Schlumberger sounding. Schlumberger sounding fails to represent the ramp structure.

### Complex Structure

The complex model shown in Fig. 15 consists of a vertical fault and three layers on one side of it. The vertical edge is located at the 101 th node.

The mapping curves for this structure in Fig. 16 are similar to those for the vertical fault. Schlumberger mapping shows clearly the vertical boundary as in the case of the vertical fault. In the case of soundings (Fig. 17), Schlumberger array shows the three layer structure while Wenner array does not.

## CONCLUSIONS

In geoelectric studies 2-D or 3-D inversions of the electric sounding data will yield a better subsurface resistivity structure than 1-D inversion. However, 2-D or 3-D inversions need more computing time and larger memory size than 1-D inversions. This study showed the 2-D geoelectric sections based on 1-D interpretations are useful in delineating simple 2-D subsurface structures.

The effectiveness of various electrode configurations such as Wenner, Schlumberger, three point and dipole-dipole arrays in delineating 2-D structures are examined. Among them, Schlumberger array proved to be superior to the other arrays in both 1-D electric sounding and mapping. Schlumberger array shows the vertical resistivity boundary very clearly, but it tends to exaggerate the resistivity near the vertical boundary. On the contrary, Wenner array fails to reveal the vertical interface clearly. The three point and dipole-dipole array shift the vertical boundary away as the potential electrode separation increases. Thus they are not suitable for 2-D interpretations. Analogous studies can be extended to 3-D model without particular difficulty.

## REFERENCES

Anderson, W.L. (1979) Computer program: Numerical integration of related Hankel transforms of orders 0 and 1 by adaptive digital filtering. Geophysics, v. 44, p. 1287-1305.

Beard, L.P. and Morgan, F.D. (1991) Assessment of 2-D

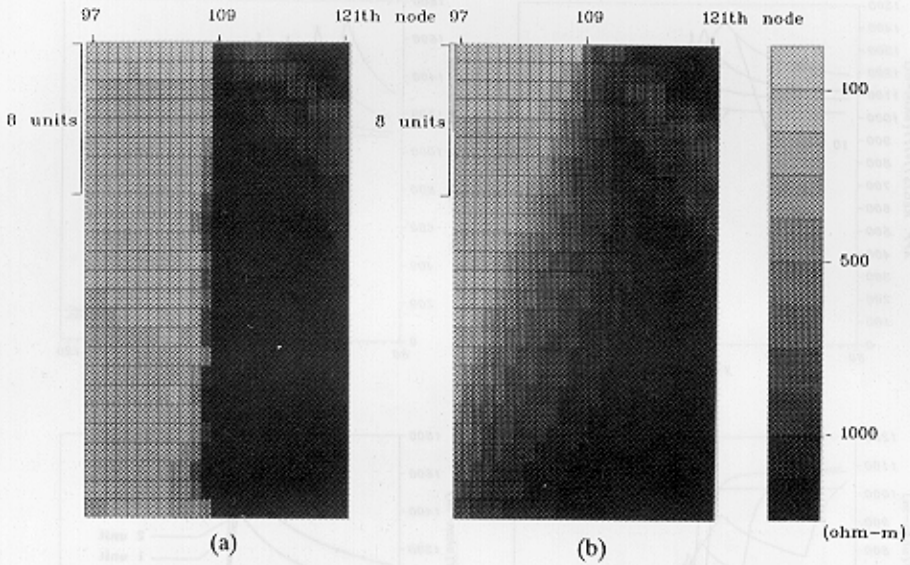


Fig. 14. 2-D cross sections for ramp model; (a) Schlumberger array (b) Wenner array.

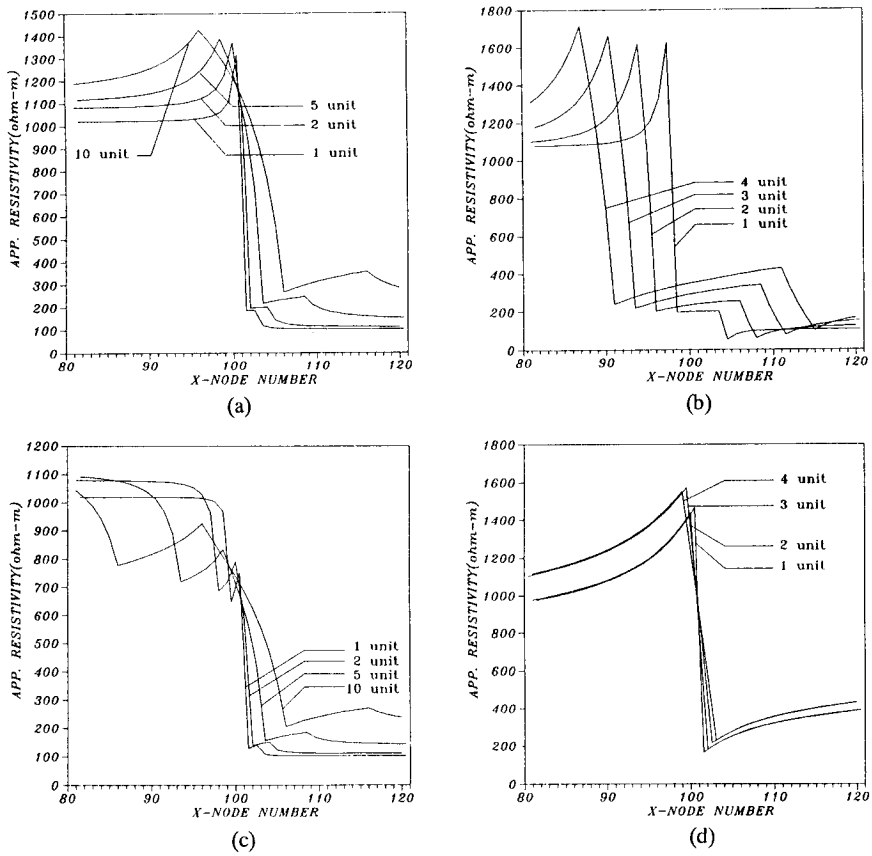


**Fig. 16.** Apparent resistivity curves of electric mappings with different potential electrode separations for complex model; (a) Three point array (b) Dipole-dipole array (c) Wenner array (d) Schlumberger array.

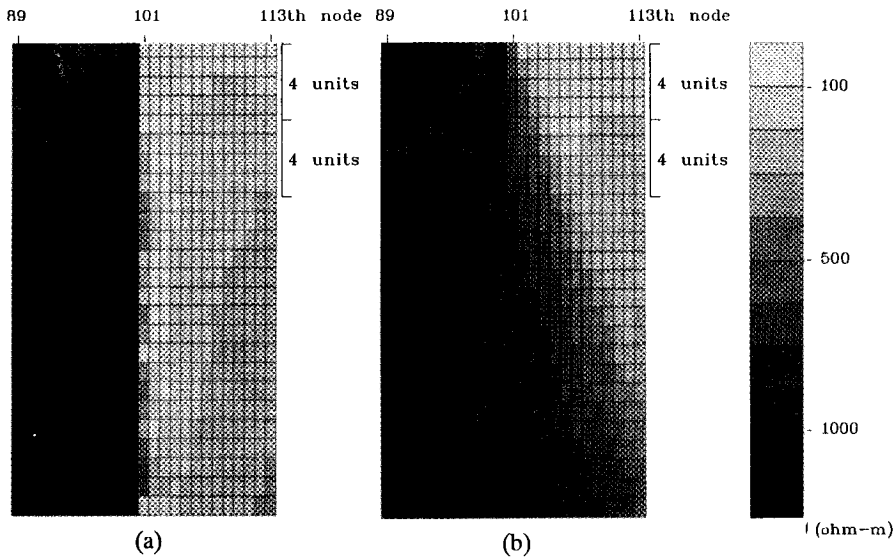


**Fig. 17.** 2-D cross sections for complex model; (a) Schlumberger array (b) Wenner array.

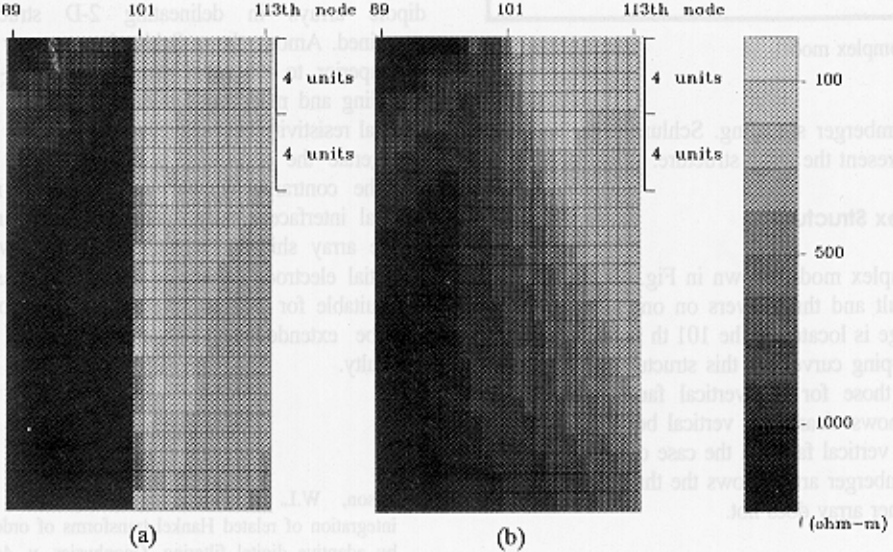


**Fig. 17.** 2-D cross sections for complex model; (a) Schlumberger array (b) Wenner array.

resistivity structures using 1-D inversion. Geophysics, v. 56, p. 874-883.

Constable, S.C., Parker, R.L. and Constable, C.G. (1987) Occam's inversion: A practical algorithm for generating smooth models from electromagnetic sounding data. Geophysics, v. 52, p. 289-300.

Dey, A. and Morrison, H.F. (1979) Resistivity modelling for arbitrary shaped two-dimensional resistivity structure. Geophysical Prospecting, v. 27, p. 106-136.

Inman, J.R. (1975) Resistivity inversion with ridge regression. Geophysics, v. 40, p. 2112-2131.

Lines, L.R. and Treitel, S. (1984) Tutorial review of least-squares inversion and its application to geophysical problems. Geophysical Prospecting, v. 32, p. 159-186.

Lowry, T., Allen, M.B. and Shive, P.N. (1989) Singularity removal: A refinement of resistivity modelling techniques. Geophysics, v. 54, p. 766-774.

Mooney, H.M., Orellana, E., Pickett, H. and Tornheim, L. (1966) A resistivity computation method for layered earth model. Geophysics, v. 31, p. 192-203.

Press, W.H., Flannery, B.P., Teukolsky, S.A. and Vetterling, W. T. (1986) Numerical recipes. Cambridge University Press.

Sasaki, Y. (1989) Two-dimensional joint inversion of magnetotelluric and dipole-dipole resistivity data. Geophysics, v. 54, p. 254-262.

Smith, N.C. and Vozoff, K. (1984) Two-dimensional DC resistivity inversion for dipole-dipole data. IEEE Tran. on Geosci. and Rem. Sens., GE-22, p. 21-28.

Telford, W.M., Geldart, L.P., Sheriff, R.E. and Keys, D.A. (1976) Applied geophysics. Cambridge University Press.

Tripp, A.C., Hohmann, G.W. and Swift, C.M. (1984) Two dimensional resistivity inversion. Geophysics, v. 49, p. 1708-1717.

Varga, R.S. (1962) Matrix iterative analysis. Prentice-Hall, Englewood Cliffs, New Jersey.

Vozoff, K. and Jupp, D.L.B. (1975) Joint inversion of geophysical data. Geophys. J. R. Astr. Soc., v. 42, p. 977-991.

Zohdy, A.A.R. (1989) A new method for the automatic interpretation of Schlumberger and Wenner sounding curves. Geophysics, v. 54, p. 245-253.

Manuscript received 6 March 1996

# 2차원 지하구조 규명을 위한 전극배열의 효율성

윤종렬 · 이기화

**요 약** : 2차원 지하구조를 해석함에 있어 1차원 역산에 근거한 수직탐사자료 해석의 타당성과 수평탐사에 있어 여러가지 전극배열법의 효율성이 연구되었다. 수직암맥, 판상기둥, 매몰수직단층, 램프 (ramp), 복합구조와 같은 2차원 모델로부터 유한차분법을 이용하여 3 포인트, 쌍극자, 베너 (Wenner), 슐럼버저 (Schlumberger) 수평탐사의 겉보기비저항 곡선을 구하고 이를 비교 분석하였다. 수직탐사의 경우에는 슐럼버저와 베너 배열법에 대하여 1차원 역산자료를 내삽하여 얻은 자료로부터 2차원 단면도를 구하여 비교하였다. 이러한 2차원 단면도는 각 모델에 대하여 비저항의 수직, 수평적인 경계면을 잘 보여주고 있다. 또한 슐럼버저 수평탐사의 겉보기 비저항 곡선은 수직적인 비저항의 경계면을 잘 보여주고 있다. 전반적으로 수직, 수평 전기탐사의 경우에 있어 슐럼버저 배열법이 다른 전극배열법보다 우수한 결과를 보여주고 있다. 본 연구로부터, 1차원 역산에 근거한 2차원 지하구조의 해석이 가능함을 알 수 있다.